

**Best
Available
Copy**

AD-A282 330
1

OFFICE OF NAVAL RESEARCH

GRANT or CONTRACT: N00014-91-J-1919

R&T Code 4133036
Robert Nowak

Technical Report No. 13

Electrochemical Atomic Layer Processing

Choong K. Rhee, Baoming M. Huang, Elvin M. Wilmer,
Sajan Thomas and John L. Stickney

In Press
for
Materials and Manufacturing Processes

Department of Chemistry
University of Georgia
Athens, GA 30602-2556

6/24/94

94-22623



Reproduction in whole, or in part, is permitted for any purpose of the United States Government.

This document has been approved for public release and sale;
its distribution is unlimited.

94 7 19 108

REPORT DOCUMENTATION PAGE

Form Approved
OMB No. 0704-0188

2. BURDEN: The burden is the cost in time and effort to collect information, estimated to average 1 hour per response, including the time for reviewing instructions, searching existing data sources, gathering and maintaining the data needed, and completing and reviewing the collection of information. Send comments regarding this burden estimate or any other aspect of this collection of information, including suggestions for reducing this burden, to Washington Headquarters Services, Directorate for Information Operations and Reports, 1215 Jefferson Davis Highway, Suite 1204, Arlington, VA 22202-4302 and to the Office of Management and Budget, Paperwork Reduction Project (0704-0188), Washington, DC 20503.

1. AGENCY USE ONLY (Leave blank)	2. REPORT DATE 6/25/94	3. REPORT TYPE AND DATES COVERED Technical - 1, June	
4. TITLE AND SUBTITLE Electrochemical Atomic Layer Processing		5. FUNDING NUMBERS G-N00014-19-J-1919	
6. AUTHOR(S) Choong K. Rhee, Baoming M. Huang, Elvin M. Wilmer, Sajan Thomas and John L. Stickney			
7. PERFORMING ORGANIZATION NAME(S) AND ADDRESS(ES) John L. Stickney Department of Chemistry University of Georgia Athens, GA 30602-2556		8. PERFORMING ORGANIZATION REPORT NUMBER Technical Report #13	
9. SPONSORING/MONITORING AGENCY NAME(S) AND ADDRESS(ES) Office of Naval Research Chemistry Division Arlington, VA 22217-5000		10. SPONSORING/MONITORING AGENCY REPORT NUMBER	
11. SUPPLEMENTARY NOTES			
12a. DISTRIBUTION AVAILABILITY STATEMENT Approved for public release and sale; its distribution is unlimited		12b. DISTRIBUTION CODE	
13. ABSTRACT (Maximum 200 words) <p>Atomic layer processing with electrochemical control is discussed. A method for the electro-deposition of compound semiconductors based on the principles of atomic layer epitaxy (ALE) is reported, with specific reference to the formation of ZnTe. This method is referred to as electrochemical atomic layer epitaxy (ECALE). A number of II-VI compounds have been formed using this method, including: CdTe, CdSe, CdS, ZnTe, ZnSe, ZnS and HgSe. Initial studies of GaAs and PbSe have also been pursued. A computer-controlled electrochemical flow deposition system is described. The system has been constructed to form thin-films of the compounds listed above using the ECALE methodology. In addition, an analogous digital electrochemical etching procedure has been developed, and used to etch CdTe substrates. The etching cycle consists of oxidizing off the top atomic layer of Cd atoms at a relatively positive potential, followed by Microscopy (AFM) has been used to image the resulting features. ECALE and the digital electrochemical etching process are both based on selecting potentials where an atomic layer of an element is deposited, or removed, in a surface limited reaction. The potentials used are referred to as underpotentials in the electrochemical literature. The atomic layer deposition process is referred to as underpotential deposition (UPD).</p>			
14. SUBJECT TERMS ECALE, CdTe, Digital etching, surfaces analysis, flow cell, electrochemistry		15. NUMBER OF PAGES 28	
		16. PRICE CODE	
17. SECURITY CLASSIFICATION OF REPORT Unclassified	18. SECURITY CLASSIFICATION OF THIS PAGE Unclassified	19. SECURITY CLASSIFICATION OF ABSTRACT Unclassified	20. LIMITATION OF ABSTRACT UL

Electrochemical Atomic Layer Processing

Choong K. Rhee, Baoming M. Huang, Elvin M. Wilmer, Sajan Thomas and John L. Stickney*.

Department of Chemistry, University of Georgia, Athens, Georgia 30602-2556.

***To whom correspondence should be addressed.**

Key words

ZnTe

CdTe

Electrodeposition

Underpotential

Electrochemical atomic layer epitaxy

ECALE

Electrochemical etching

Digital etching

Atomic force microscopy

AFM

Scanning tunneling microscopy

STM

Thick layer cell

Thin layer cell

Flow cell

ABSTRACT

Atomic layer processing with electrochemical control is discussed. A method for the electrodeposition of compound semiconductors based on the principles of atomic layer epitaxy (ALE) is reported, with specific reference to the formation of ZnTe. This method is referred to as electrochemical atomic layer epitaxy (ECALE). A number of II-VI compounds have been formed using this method, including: CdTe, CdSe, CdS, ZnTe, ZnSe, ZnS and HgSe. Initial studies of GaAs and PbSe have also been pursued. A computer-controlled electrochemical flow deposition system is described. The system has been constructed to form thin-films of the compounds listed above using the ECALE methodology. In addition, an analogous digital electrochemical etching procedure has been developed, and used to etch CdTe substrates. The etching cycle consists of oxidizing off the top atomic layer of Cd atoms at a relatively positive potential, followed by reducing off the top layer of Te atoms at a relatively negative potential. Atomic Force Microscopy (AFM) has been used to image the resulting features. ECALE and the digital electrochemical etching process are both based on selecting potentials where an atomic layer of an element is deposited, or removed, in a surface limited reaction. The potentials used are referred to as underpotentials in the electrochemical literature. The atomic layer deposition process is referred to as underpotential deposition (UPD).

Introduction

Atomic Layer Epitaxy (ALE) is a deposition methodology in which a cycle is used to deposit compounds "digitally", one monolayer at a time (1-4). Although ALE has been developed primarily as an application of Chemical Vapor Deposition (CVD) or Molecular Beam Epitaxy (MBE), the principles have recently been applied in the electrochemical deposition of compound semiconductors (5-9). As in ALE, Electrochemical Atomic Layer Epitaxy involves a deposition cycle, at separate potentials, in the ECALE cycle. Atomic layers of each element are deposited from separate solutions. Deposition is limited to an atomic layer by using underpotentials to deposit each element. Underpotential deposition refers to a phenomenon where, due to the heat of compound formation, one element deposits on a second element at a potential prior to (under) that necessary to deposit the element on itself (10). Classically, UPD has been associated with the deposition of one metal on a second, which is referred to here as reductive UPD (10). In addition, there are a number of systems where oxidative UPD is observed. This involves the deposition of an atomic layer of an element by oxidation of a reduced form of the element. Again, an atomic layer of the element deposits at a potential prior to that needed to deposit the element on itself. Examples of oxidative UPD include: I onto Au (11), oxygen onto Cu (12), As onto Au (8), and Te onto Au (13).

The ECALE methodology requires an exchange of solution after the deposition of each component element. Each element is deposited from a solution designed specifically for the deposition of that element. The solution pH is a major variable. Blank solutions, corresponding to the deposition solutions, are used between the deposition solutions. In this way, the precursor to one element can be flushed out of the cell with its corresponding blank solution prior to introduction of solutions containing precursors to the subsequently depositing elements.

Presently, deposits are formed in a thin-layer electrochemical cell (14). Thin-layer cells are used for a number of reasons: they keep the quantity of solution (1-10 $\mu\text{L cm}^{-2}$) needed for a given deposition step to a minimum; the lower volumes of solutions result in lower amounts of any solution-born contaminants; and thin-layer cells can be designed to facilitate exchange of the solution in contact with the electrode.

Manual thin-layer cells have been used extensively in ECALE studies. Due to the large number of steps making up each ECALE cycle, however, use of a manual thin-layer cell becomes tedious and reproducibility drops, especially for deposits formed with more than 10 cycles. A computer-controlled electrochemical thin-layer flow-cell is presently being used to form deposits with more than 10 cycles.

In addition to compound formation using the ECALE methodology, an electrochemical form of "Digital Etching" (15) has been developed in this group (16). The process is essentially the inverse of ECALE, in that UPD potentials are used as stripping potentials for the individual elements in a compound. That is, a low potential is first used to reduce off the top layer of one element, by forming a soluble anionic species. A more positive potential is then used to oxidize off the top layer of the other element, by forming a soluble cationic species. Pure electrolyte is continuously flushed over the substrate to rinse away the product ions. Only the top layer of an

element is removed in this procedure, since the potential is kept below that needed to strip the element from the bulk of the compound, where the element is fully coordinated.

Table 1. Status of compound formation by ECALE.

II-VI	O	S	Se	Te
Zn	YES?	YES	YES	YES
Cd	YES	YES	YES	YES
Hg	YES	U		

IV-VI	O	S	Se	Te
Sn	P	P	P	
Pb	P	YES	U	

III-V	N	P	As	Sb	Bi
Al					
Ga		YES?		P	
In		P		P	
Tl		P		P	

P=Probably, but has not yet been investigated

U=Under investigation; ?=Not yet clear, but has been studied

Initial ECALE studies have centered on investigations of CdTe deposition (5-7). Subsequent work has taken a number of directions, including fundamental atomic level studies of the growth of the first two monolayers of CdTe on Au single crystals (13, 17, 18). ECALE cycles are being developed for the deposition of other compounds as well. Cycles have been developed for CdTe (5-7), GaAs (7, 8), CdS (19), CdSe, ZnSe, and PbSe (Table 1). Recent studies of ZnTe deposition are presented in this article.

Experimental

A diagram of the electrochemical flow-cell system used for ECALE deposition is shown in FIG. 1. A simplified version of the same instrument may be used for digital electrochemical etching. It consists of a thin-layer electrochemical flow-cell, interfaced to a distribution valve. PEEK tubing is used to plumb the system, due to its low oxygen permeability. Distribution valves with four or six inlets and a single outlet were used, as two solutions are needed for each element deposited. The solutions used to deposit a given element have their pH and supporting electrolyte

optimized for the deposition of that element. A corresponding blank solution was also used in order to rinse away excess reactant prior to introduction of the next reactant solution. The four-way valve was used for the formation of binary compounds, while a new system uses a six-way valve in order for three elements to be deposited. This system will be used for the formation of ternary compounds, superlattices, and for doping studies.

Because the cell volumes were on the order of 10 mL or less, accurate pumping was required. Microliter pipeting pumps designed to deliver aliquots of 2 to 25 mL in a single shot, or small parastaltic pumps were used. The solution reservoirs were made with Pyrex glass bottles and Teflon valves.

The design of the flow-cell (FIG. 1) is similar to those available commercially. The face plate of the cell was made of Plexiglass, since it allowed visual inspection of the depositing films. A Teflon gasket, 0.005" thick, with an oblong hole sufficient to encompassing the inlet and outlet, was placed on the inside of the Plexiglass face plate. The inlets and outlets were tapped 1/4-28 for attachment of the plumbing.

The substrates were 0.010" Au foil and were supported by a Plexiglass or stainless steel block which swiveled on the end of a bolt with a hemispherical head. A torque wrench was used to reproducibly tighten the bolt and compress the cell. The bolt was set in a stainless steel U-block (FIG. 1). A separate compartment, attached to the cells' exit stream, was used for the reference and auxiliary electrodes. The compartment was separated from the flow stream by a porous Vicor plug.

Manual thin-layer electrochemical cells were used, as well (6). These electrodes consist of an Au rod set in a fitted glass cavity. The glass walls were designed to be on the order of 0.001" from the Au rod. Two pin holes were ground into the bottom of the glass in order for the solution to be flushed in and out of the thin-layer cavity. In addition, the holes provide a path for ionic conductivity. Cell volumes were on the order of 3-4 mL, for an electrode area of 1-1.4 cm². Application of a slight excess of N₂ pressure inside the cell, flushes solution from the cell. If the cell is then placed in contact with a new solution, and the N₂ pressure is released, an aliquot of the new solution will wick into the cell by capillary action. The result is a complete exchange of solution, a rinse.

Solutions were prepared with water from a Nanopure water filtration system, fed from the house deionized water supply, and analytical grade reagents. The potentiostats were built in-house using a conventional op-amp based design. All potentials are reported versus the Ag/AgCl (1M NaCl) reference electrode.

Results and Discussions

ZnTe Formation

The formation of ZnTe serves an example of electrochemical ALE. FIG. 2 is a series of cyclic voltammograms depicting the deposition of Zn and Te on polycrystalline Au in a manual thin-layer electrochemical cell. FIG. 2a is a scan of the clean Au electrode in 1 M H₂SO₄. The basic features of the voltammogram are the oxidation of the Au surface at high potentials and the subsequent reduction of the Au oxide on the negative going scan. Hydrogen evolution is visible as the negative limit of the voltammogram. A negative scan from the rest potential with an aliquot of a 0.25 mM TeO₂ solution, pH 3, is shown in FIG. 2b. A UPD peak at 0.25 V and a bulk deposition peak at -0.05 V are evident in the voltammetry. The negative limit in the voltammetry corresponds to hydrogen formation. FIG. 2c is voltammetry for the Au electrode covered with two monolayers of Te in a borate solution buffered at pH 8.6. A distinct feature is visible at -1.0 V, corresponding to the reduction bulk Te to telluride ion, Te²⁻. Reversal of the scan direction results in the reoxidation of the Te²⁻ to Te. Studies have shown (5) that rinsing with a blank solution at potentials below -1.1 V removes the Te²⁻, leaving only an atomic layer of Te (dashed curve in FIG. 2c). This process is referred to as oxidative Te UPD. Oxidative Te UPD involves the reaction:



as opposed to reductive Te UPD which involves the reaction:



Ideally, a species such as Te²⁻ would be used for the formation of atomic layers of Te by oxidative UPD in the EC.ALE formation of Te containing compounds. The instability of Te²⁻ containing solutions, however, makes this impracticable. This procedure does work in the EC.ALE formation of sulfur containing compounds (19). Solutions of S²⁻ are stable and can be oxidized to form sulfur atomic layers. Oxidative UPD of both Se and Te are, however, performed inversely. Instead of oxidizing an atomic layer of Te onto the surface from a Te²⁻ solution, bulk Te is first deposited by reduction from a HTeO₂⁺ solution. Excess (bulk) Te is then reductively stripped away in a blank solution, leaving an atomic layer of Te.

After the formation of a Te atomic layer, Zn was deposited by exchanging the solution for 10 mM ZnSO₄ and reducing at -1.0 V. FIG. 2d displays the voltammetry associated with the deposition of Zn on an atomic layer of Te. At -0.7 V a shoulder appears, which corresponds to reductive Zn UPD on the Te. At more negative potentials a steeply increasing reduction current is observed, which corresponds to the deposition of bulk Zn and the evolution of H₂.

Voltammetry, such as that in FIG. 2, was used to develop an EC.ALE cycle for the formation of ZnTe. The cycle started with Te deposition at -1.0 V from a 0.4 mM TeO₂ solution, borate buffered at pH 8.6 with 1 M NaClO₄, as a supporting electrolyte. The solution was then

exchanged for an equivalent blank solution, containing no TeO_2 , and rinsed three times at -1.30 V, completing oxidative Te UPD.

Zn was then deposited from a 10 mM ZnSO_4 solution, buffered with phthalate at pH 5.2 and containing 0.5 M Na_2SO_4 as a supporting electrolyte with the potential poised at -1.0 V. The cycle was completed by rinsing with the corresponding Zn blank solution three times

Studies of the coverages of Zn and Te resulting from differing numbers of cycles, up to 16, were performed using a manual thin-layer cell. Coverages were determined in-situ by electrochemically stripping the resulting deposits. FIG. 3 displays the stripping voltammetry, for deposits formed from 2, 8 and 16 ECALE cycles, in 0.5 M Na_2SO_4 + 0.5 M phthalate. There are four oxidation features visible in the stripping scan. The first two, at -0.6 and -0.2 V, correspond to the stripping of Zn from the deposit in a two electron process forming Zn^{2+} . The second two, at 0.1 and 0.4 V, correspond to the oxidation of the Te to HTeO_2^+ in a four electron process (eq. {2}). Zn and Te coverages were obtained by integration of the peak areas, and the data are shown in FIG. 4. The lattice constant for ZnTe is 0.61 nm, whereas twice the Au-Au distance in the Au(100) plane is 0.584 nm, resulting in a 4% lattice mismatch. If we assume epitaxial deposition on the Au surface with a 4% contraction in the ZnTe lattice, one cycle should result in the deposition of a 1/2 monolayer of Zn and a 1/2 monolayer of Te, where a monolayer refers to the number of surface Au atoms. The solid line shown in FIG. 4 corresponds to the deposition of 1/2 monolayer per ECALE cycle. The surface area of the electrode was taken to be the geometric surface area multiplied by a roughness factor of 1.2. The average Au surface atomic density for the polycrystalline Au electrode was taken to be that of a Au(100) surface, 1.2×10^{15} atoms/cm². Experience has shown these assumptions to hold for similar electrodes within about 10%.

For deposits made with less than about 10 cycles, the Zn coverage is a little high relative to the 1/2 monolayer per cycle line, while the Te coverage is a little low (FIG. 4). At 16 cycles, both Te and Zn coverages are low by about 15% relative to the 1/2 monolayer/ cycle line. The reasons for the initially high Zn coverage appear to be related to the first Zn oxidation peak. It is well formed, after only 2 cycles (FIG. 3a), and it remains nearly constant in size as the number of cycles increases. After the second cycle, it is only the second Zn stripping peak at -0.2 V which continues to grow.

The nature of the first Zn stripping peak is not clear. It is expected that the top layer of Zn will oxidize off at a less positive potential than Zn completely coordinated to Te in the deposit. The first Zn stripping peak, however, corresponds to more than the 1/2 monolayer of Zn expected for stripping the top Zn atomic layer.

After 10 cycles, the curves for Zn and Te both drop down, relative to the 1/2 monolayer per cycle line. The reasons for this are also not clear. The potentials needed for optimal 1/2 monolayer deposition may vary as the deposit grows. It may simply be increased operator error. Depositing 16 cycles with a manual thin-layer cell is very tedious. The trend in coverage per cycle will be the subject of future studies using the computer-controlled flow-cell described in the next section. Besides operator error or a change in the optimal deposition potentials, examination of FIG. 3c shows that the base line resolution between Zn stripping and Te stripping, is disappearing

at the 16 cycle level. In addition, it is probably difficult to completely strip the Zn from a deposit made from 16 cycles. If, however, not all the Zn was stripped by the completion of the second Zn stripping peak, it would be expected to oxidize during the Te stripping features, increasing the observed Te stripping charge. The Te charge, however, decreased as well.

Flow-cell

As mentioned, the use of a manual thin-layer cell for more than about 10 cycles, proves tedious. The computer-controlled flow-cell deposition system, described in the experimental section (FIG. 1), is presently being used to form thicker deposits without the operator error inherent in manual thin-layer studies. FIG 5 describes the program used to deposit CdTe in the flow-cell deposition system. Prior to application of the ECALe cycle, the 0.01" Au foil substrates were cleaned by etching in nitric acid and then annealed in a gas oxygen flame. The cell was then assembled and torqued together. Voltammetric cycles were run in 1 M H_2SO_4 , in order to assure substrate cleanliness, prior to initiation of the deposition program.

The program in FIG. 5 was the first used to make CdTe deposits with the flow cell. The ECALe cycle (FIG. 5) began with the introduction of the $HTeO_2^+$ solution at open circuit. Open circuit was used in order to avoid depositing most of the Te at the entrance of the cell. Five 15 μL aliquots of the $HTeO_2^+$ solution were used to exchange the system volume, where the system volume includes the solution in the outlet of the distribution valve, in the cell, and in the tubing leading up to the cell. After the $HTeO_2^+$ solution was introduced to the cell, it was held quiescent while deposition was carried out at -0.8 V, a potential where all $HTeO_2^+$ present in the cell was deposited. The cell volume was sufficiently small that only a few monolayers of Te were deposited. The electrode potential was then allowed open circuit, while the system volume was flushed with the Te blank solution, removing any remaining $HTeO_2^+$. If the potential had been held at -0.8 V while the remaining $HTeO_2^+$ was flushed through the cell, the $HTeO_2^+$ present would have deposited at the entrance to the cell, and would have proven difficult to remove. The potential was next shifted to -1.25 V and held, filled with the blank solution. Bulk Te is unstable at -1.25 V, forming Te^{2-} which is soluble. The cell was then flushed out multiple aliquots of the Te blank solution. The Cd blank solution was then introduced and the potential shifted to -0.6 V, the Cd UPD potential. The Te and Cd deposition solutions differed by several pH units, and use of the Cd blank solution served to condition the tubing and cell, prior to introduction of the Cd solution itself. This prevented $Cd(OH)_2$ formation. The $CdSO_4$ solution was then introduced and Cd was deposited at -0.6 V, with the solution quiescent. Finally, excess $CdSO_4$ was swept from the cell using aliquots of the Cd blank solution followed by the Te blank solution, and the cycle was begun again.

FIG. 6 depicts Cd and Te coverages, and the Te/Cd ratio, for deposits made with 50 ECALe cycles, as a function of the Cd UPD potential. The coverages are relative, determined using Electron Probe Micro Analysis (EPMA). Some ICP-AES experiments were performed to obtain absolute Cd coverages, however. Selected deposits were dissolved in nitric acid and analyzed for total Cd contents. These results were then used to calibrate the EPMA data. At Cd potentials above -0.5 V, a sharp drop-off in Cd coverage is observed. The Te coverage drops as well, pointing out the dependence of the Te coverage on the presence of Cd at the surface. The

Te/Cd ratio was a little high at -0.4 V, as well, but the stoichiometry is still 1:1. A plateau is evident between -0.6 V and -0.7 V, at a coverage very close to the predicted 1/2 monolayer of Cd and 1/2 monolayer of Te per cycle. At the most negative potential, -0.8 V, the coverages of both the Cd and Te increased significantly. This increase was anticipated, as bulk Cd begins to deposit in this potential range. It is interesting to note, however, that the stoichiometry remains 1:1 over the entire range of Cd deposition potentials studied.

Deposits of CdTe have been formed using the program in FIG. 5 with from 10 to 100 cycles. FIG. 7a is a diagram of the surface coverages of Cd and Te in CdTe deposits made with increasing numbers of cycles, determined in arbitrary units with EPMA. FIG. 7b shows that the stoichiometry of the deposits, again, remains close to 1:1, as the number of cycles is increased. The relative Te coverage, however, drops a little after 100 cycles. A dramatic increase in the slope of the graph above 50 cycles indicates that the coverage per cycle is increasing for these thicker deposits. The cause of this increase is clearly seen in the electron micrographs shown in FIG. 8. At 50 cycles, a series of 100-200 nm particles appear. As the number of cycles is further increased, clumps of particles are observed. Evidently, the increased coverages at high cycle numbers is the result of an exponential increase in surface area due to increased surface roughness. Again, it is interesting to note that the stoichiometry of the deposits remains nearly 1:1, even while the surface is roughening.

Presently, the causes of the formation of these particles are under investigation. One line of investigation underway in our group involves STM studies of islands on the Au substrates. These islands appear to be formed during the electrochemical cleaning cycles, prior to deposition. FIG. 9 is a STM micrograph of some of these islands. Their heights correspond to atomically high Au islands. The increased number of surface defects associated with the presence of these islands may contribute to the nonideal deposit morphology. The islands appear to be the result of the formation and removal of surface reconstructions on the Au (20, 21). The reconstructed surfaces are formed upon annealing and involve a higher surface density of atoms. Positive potentials used during the cleaning cycles, serve to lift the reconstructions, freeing up the excess surface atoms. The result is that the excess Au atoms coalesce into islands. Another likely source of the observed particles involves unflushed solution volumes in the cell, tubing, or valves. If Te²⁻ formed during the cycle comes in contact with solution containing Cd²⁺, they can homogeneously precipitate and adsorb on the deposit surface. These adsorbed particles could then act as nucleation centers. Work with the cell design and rinsing procedures are under way to try and eliminate this possibility.

Digital Electrochemical Etching

Besides studies of ECALe deposition, digital electrochemical etching of compound semiconductors is being pursued (16). The electrochemical program used is essentially the inverse of the ECALe deposition program. The principle, for a compound semiconductor, is that the top layer of atoms is less strongly bound to the substrate than are atoms of the same element buried deeper in the compound, that are more coordinatively saturated. It should be possible to remove this top layer of atoms at a lower potential than that required to strip atoms of the same element in the bulk of the compound. To digitally etch CdTe, a relatively positive potential is

used to oxidize the top layer of Cd atoms, but not positive enough to strip Cd from the bulk of the CdTe lattice. The Cd²⁺ ions formed are then flushed away, leaving a layer of Te atoms as the top atomic layer. Next, a relatively negative potential is used to reduce the top layer of Te atoms to Te²⁻ ions, which are flushed away. Studies in aqueous solutions have shown that it is very difficult to reduce Te from the bulk of CdTe, regardless of how negative a potential is used. The net result of the reduction is to remove the top atomic layer of Te, leaving a Cd terminated surface.

The potential used to oxidize the top atomic layer of Cd atoms is one of the more important variables in the etching cycle. The dependence of etched depth on the Cd stripping potential is discussed below.

A thin-layer flow-cell system, similar to that shown in FIG. 1, has been used in most of the digital electrochemical etching studies performed thus far. It is important to completely flush product ions from the surface prior to changing the stripping potential. If the ions produced are not completely flushed away, they can redeposit during the subsequent half cycle, probably contributing to surface roughening. A CdTe (100) crystal (II-VI Inc.) was used as the substrate in the present studies. An ohmic contact was made on the back using high purity In and a Al foil. The etching solution used contained 0.1 M Na₂SO₄, pH 5.7. The pH 5.7 was high enough to allow Te²⁻ based species to form at -1.3 V without excessive hydrogen evolution, yet it was low enough to avoid Cd(OH)₂ formation.

Separate stripping solutions could have been used for the two cycle halves, if it were deemed advantageous. The potentiostat was computer interfaced, although a simple function generator would have been sufficient. The flow rate of the solution was a constant 1.1 mL/min.

The voltammetry in FIG. 10 is for the CdTe crystal in a thick layer cell. Both the oxidation of Cd at 0.3 V and the reduction of Te at -1.0 V are visible in the voltammetry. Use of a potential less than -1.0 V for stripping the Te atomic layers appears reasonable from examination of FIG. 10. The potential needed to strip the top layer of Cd was not as clear cut.

A separate set of experiments was performed, as a function of the Cd stripping potential, using a thick-layer cell. The charge for the subsequent reduction of the top layer of Te atoms was used to determine the extent of Cd removal. The idea was that if the Cd stripping potential were too low, insufficient Cd would be removed and the subsequent reduction charge for Te would be low. If the Cd stripping potential were too high, the Te reduction charge would be too high. FIG. 11 is a graph of the resulting charges for Te stripping. Those experiments were problematic, as the background corrections were very difficult to make. The substrate used was a piece of p-CdTe(100) with a band gap of 1.5 eV, thus the background at potentials where Te²⁻ was formed shifted significantly from run to run due to minor changes in room light. These difficulties are reflected in the scattering of the data (FIG. 11). However, a distinct S curve, with a plateau between 0.05 V and 0.35 V is evident.

In order to obtain a more accurate measure of the amounts of material removed per etching cycle, a second set of data on digital etching was obtained using AFM. The depth sensitivity of AFM is optimal for surface profiling substrates with features on the order of 50 nm

to 200 nm deep. To use the AFM effectively, however, the surface had to be patterned. With the surface patterned, etching produced an ordered series of micron sized features. Profiles were then used to determine etched amounts. A positive photo-resist system, AZ-1350, from Hoechst Celanese was used to form the patterns.

FIG. 12 is an AFM micrograph of the surface of a digitally etched CdTe(100) surface. The crystal was initially etched in a Br_2 -methanol solution prior to application of the photo-resist. It was exposed using a test mask and developed leaving the photo-resist pattern on the surface. The crystal was then incorporated into a thin-layer electrochemical flow-cell, as described above, and 300 etching cycles were performed. A surface profile drawn across an etched features is shown in FIG. 13. The etched depth appears to be 137 nm, or 0.46 nm/cycle. Based upon the lattice constant of zinc blende CdTe, which is 0.648 nm, one monolayer should be 0.324 nm thick. The ideal one cycle etch depth should thus be 0.324 nm/cycle. These are the first AFM images of digitally electrochemically etched substrates. Presently, studies are underway to examine the dependence of the amount etched per cycle versus the following cycle variables: Cd etching potential, Te etching potential, flow rate, and solution composition. Besides optimizing the amount etched per cycle, the morphology of the resulting etched surfaces will be examined, as well as any anisotropy in the etch walls or surfaces.

Acknowledgements

Acknowledgment is made to the Department of the Navy, Office of the Chief of Naval Research, under Grant No. N00014-91-J-1919. Acknowledgment is also made to the National Science Foundation for partial support of this work under Grant No. DMR-9017431.

References

- (1) Suntola, T. and Antson, J., Finnish Patent No. 52359 (1974); U.S. Patent No. 4058430.
- (2) Nishizawa, J.-I., Abe, H., and Kurabayashi, T., *J. Electrochem. Soc.*, Vol. 132, p.1197(1985); Goodman, C.H.L. and Pessa, M.V., *J. Appl. Phys.*, Vol. 60, R65 (1986); DenBaars, S.P. and Dapkus, P.D., *J. Cryst. Grow.*, Vol. 98, p.195(1989).
- (3) Kuech, T.F., Dapkus, P.D., and Aoyagi, Y., "Atomic Layer Growth and Processing", MRS, Pittsburgh, Vol. 222, 1991; Bedair, S., "Atomic Layer Epitaxy," Elsevier Sci., Amsterdam, 1992.
- (4) Niinisto, L. and Leskela, M., *Thin Solid Films*, Vol. 225, p.130(1993).
- (5) Gregory, B.W. and Stickney, J.L., *J. Electroanal. Chem.*, Vol. 300, p.543(1991).
- (6) Gregory, B.W., Suggs, D.W., and Stickney, J.L., *J. Electrochem. Soc.*, Vol. 138, p.1279(1991).
- (7) Suggs, D.W., Villegas, I., Gregory, B.W., and Stickney, J.L., in "Atomic Layer Growth and Processing", Eds. Aoyagi, Y., Dapkus, P.D. and Kuech, T.F., MRS, Pittsburgh, Vol. 222, p283(1991).
- (8) Villegas, I. and Stickney, J.L., *J. Electrochem. Soc.*, Vol. 139, p.686(1992).
- (9) Stickney, J.L., Villegas, I., Gregory, B.W., and Suggs, D.W., *J. Vac. Sci. Technol. A*, Vol. 10, p.886(1992).
- (10) Kolb, D.M., in "Advances in Electrochemistry and electrochemical Engineering", Eds. Gerischer, H. and Tobias, C.W., John Wiley and Sons, New York, p125(1978); Jutter, K. and Lorenz, W.J., *Z. Phys. Chem. N.R.*, Vol. 122, p.168(1980).
- (11) Villegas, I., Suggs, D.W., Stickney, J.L., Bravo, B.G., and Soriaga, M.P., *J. Phys. Chem.*, Vol. 95, p.5245(1991).
- (12) Droogs, J.M.M. and Schlenter, B., *J. Electroanal. Chem.*, Vol. 112, p.387(1980).
- (13) Suggs, D.W. and Stickney, J.L., *J. Phys. Chem.*, Vol. 95, p.10056(1991).
- (14) Hubbard, A.T., *Crit. Rev. Anal. Chem.*, Vol. 3, p. 201(1973).
- (15) Meguro, T. and Aoyagi, Y., in "Atomic Layer Growth and Processing", Eds. Kuech, T.F., Dapkus, P. D and Aoyagi, Y., MRS, Pittsburgh, Vol. 222, p121(1991); Sakaue, H., Asami, K., Ichihara, T., Ishizuka, S., Kawamura, K. and Horiike, Y., *ibid*, p195; Aoyagi, Y., Shimura, K., Kawasaki, K., Nakamoto, I., Gamo, K. and Namba, S., *Thin Solid Films*, Vol. 225, p.120(1993);

Yamamoto, J., Kawasaki, T., Sakaue, H., Shingubar, S. and Horiike, Y., Thin Solid Films, Vol. 225, p.124(1993), Meguro, T., Ishii M., Kodama, K., Yamamoto, Y., Gamo, K., and Aoyagi, Y., Thin Solid Films, Vol. 225, p.136(1993).

(16) Lei, Q.P. and Stickney, J.L., in "Interfacial Dynamics and Growth", Eds. K.S. Liang, Anderson, M.P., Bruinsma, R.F. and Scoles, G., MRS, Pittsburgh, Vol. 237, 335(1992).

(17) Suggs, D.W. and Stickney, J.L., Surf. Sci., in press.

(18) Suggs, D.W. and Stickney, J.L., Surf. Sci., in press.

(19) Teklay, D., Colletti, L.P., and Stickney, J.L., J. Electroanal. Chem., submitted.

(20) Nichols, R.J., Magnussen, O.M., Hotlots, J., Twomey, T., Behm, R.J., and D. M. Kolb, D.M., J. Electroanal. Chem., Vol. 290, p.21(1991).

(21) Gao, X., Hamelin, A., and Weaver, M.J., Phys. Rev. B, Vol. 46, p.7096(1992).

FIGURE CAPTIONS

FIG. 1. Schematic diagram of the electrochemical thin-layer flow-cell system.

FIG. 2. Cyclic voltammograms in TLE. (a) Clean Au electrode in 1 M H_2SO_4 . (b) Clean Au electrode in 0.25 mM TeO_2 + 20 mM H_2SO_4 + 0.5 M Na_2SO_4 , pH=2.9. (c) Au electrode covered with two monolayers of Te in 10 mM borate buffer + 1 M NaClO_4 , pH=8.6. (d) Au electrode covered with an atomic layer of Te in 10 mM ZnSO_4 + 3.9 mM NaOH + 0.5 M potassium hydrogen phthalate buffer + 0.5 M Na_2SO_4 , pH=5.2.

FIG. 3. Stripping voltammetry for ZnTe deposits, in 3.9 mM NaOH + 0.5 M potassium hydrogen phthalate buffer + 0.5 M Na_2SO_4 , pH=5.2. (a) 2 cycles, (b) 8 cycles and (c) 16 cycles.

FIG. 4. Graphs of number of monolayers of Zn (triangle) and Te (square) versus the number of ECALe deposition cycles. Solid line represents the theoretically ideal 1/2 MONOLAYER/cycle line.

FIG. 5. Program of potentials and solution amounts in one ECALe cycle for CdTe deposition.

FIG. 6. Graphs of the amount of Cd (open circle) and Te (cross) in deposits, determined using EPMA, as a function of the Cd deposition potential. Filled circles represent the ratio of Te/Cd.

FIG. 7. Graphs of the amounts of Cd (open circle) and Te (cross) in deposits, determined with EPMA, as a function of the number of ECALe cycles. Filled circles represent the ratio of the amount of Te/Cd.

FIG. 8. SEM micrograph of CdTe deposits on Au, formed with different numbers of ECALe cycles: a) 20; b) 50; c) 75; d) 100.

FIG. 9. A STM micrograph of Au islands formed on Au(100) surface, after removal of the surface reconstruction.

FIG. 10. A thick-layer cell voltammogram of p-type CdTe(100) in 0.1 M Na_2SO_4 , pH=5.7.

FIG. 11. Dependence of reductive Te stripping charge, on CdTe(100), on the potentials used for oxidative Cd stripping in 0.1 M Na_2SO_4 , pH=5.7. A Cd was oxidized for one minute.

FIG. 12. An AFM micrograph of a CdTe(100) surface after 300 digital etching cycles. The etching was performed in 0.1 M Na_2SO_4 using 0.3 V and -1.3 V for Cd and Te stripping, respectively. The etching times were 1 minutes at each potential, and the flow rate of solution was 1.1 monolayer/min.

FIG. 13. The surface profile of a CdTe feature, formed by digitally etching 300 cycles.

Figure 1 Choong K. Rhee et. al.

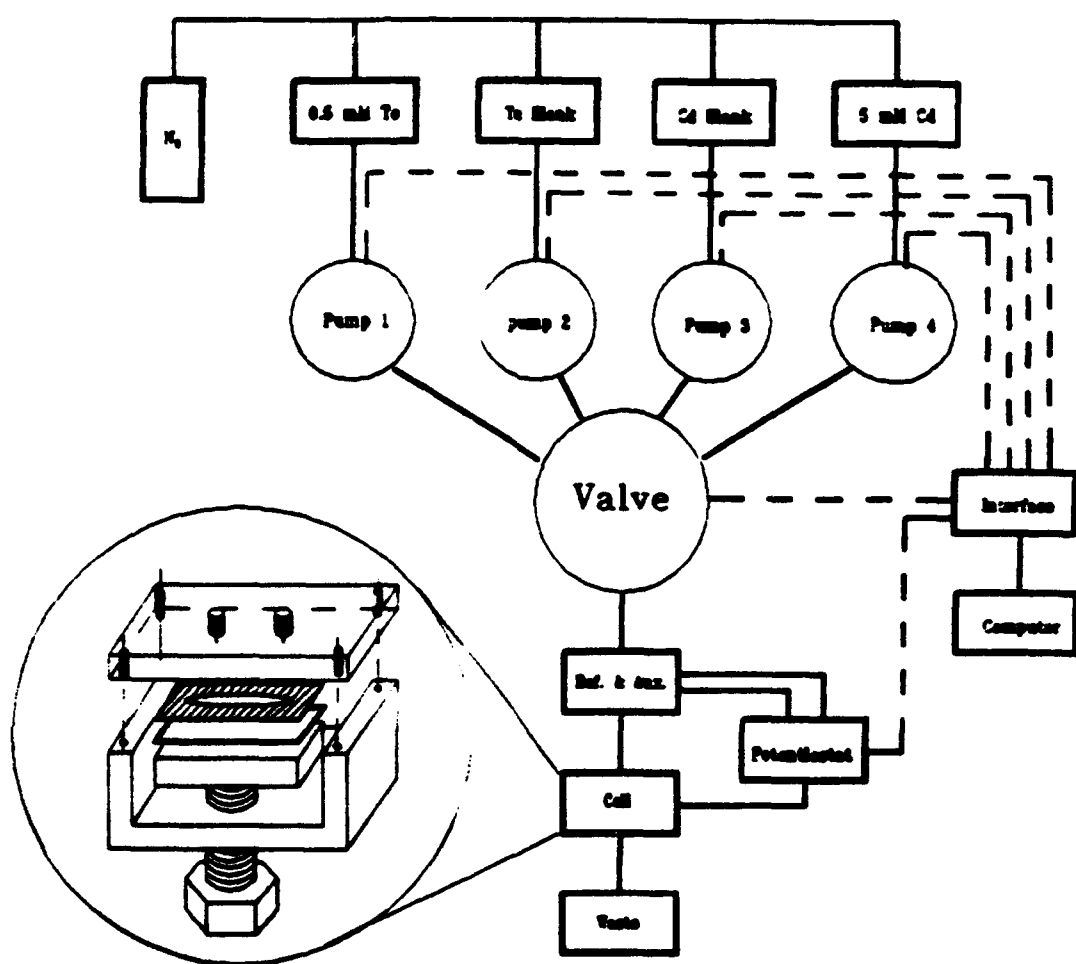


Figure 2. Choong K. Rhee et al.

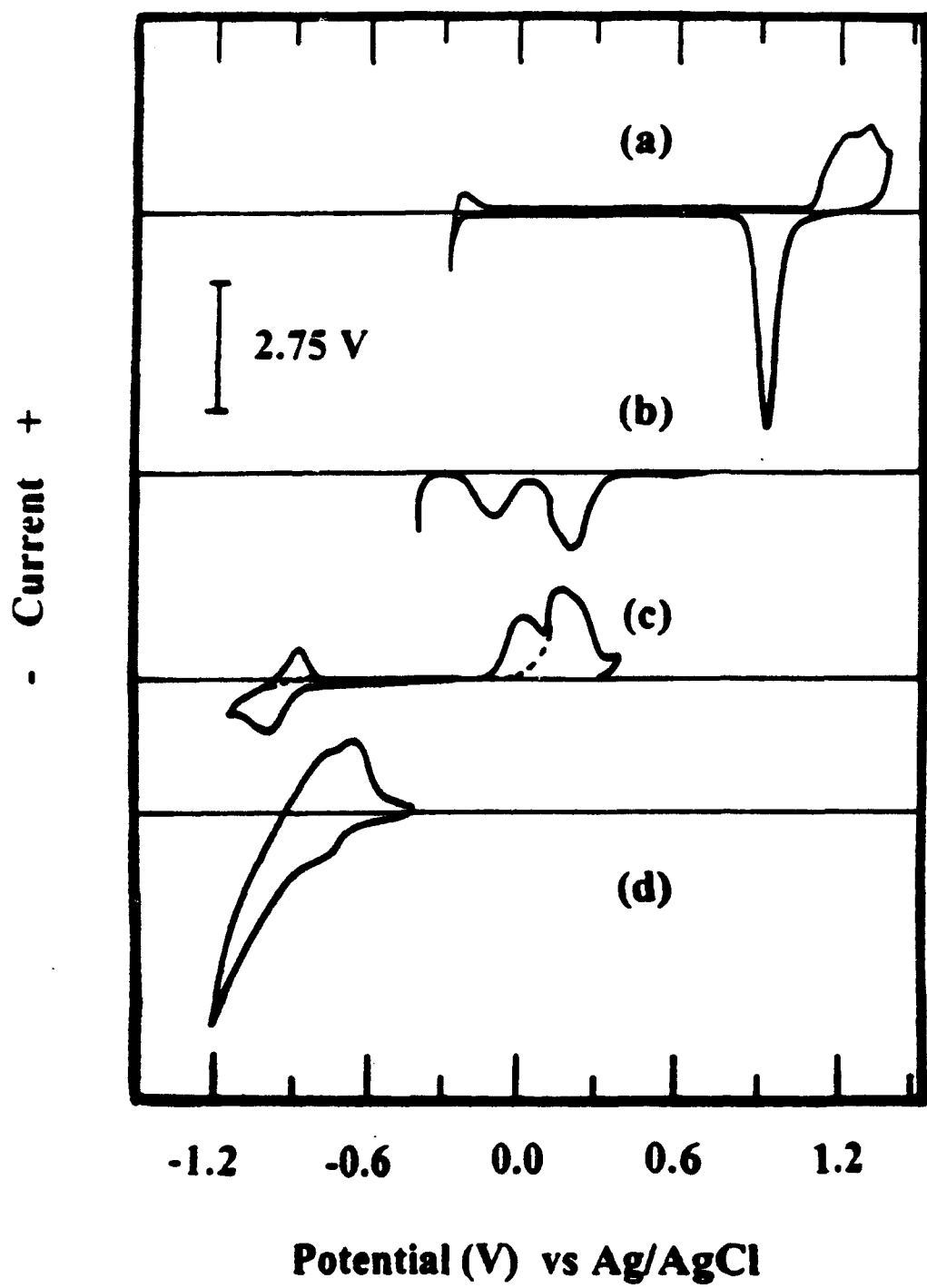


Figure 3 Choong K. Rhee et al.

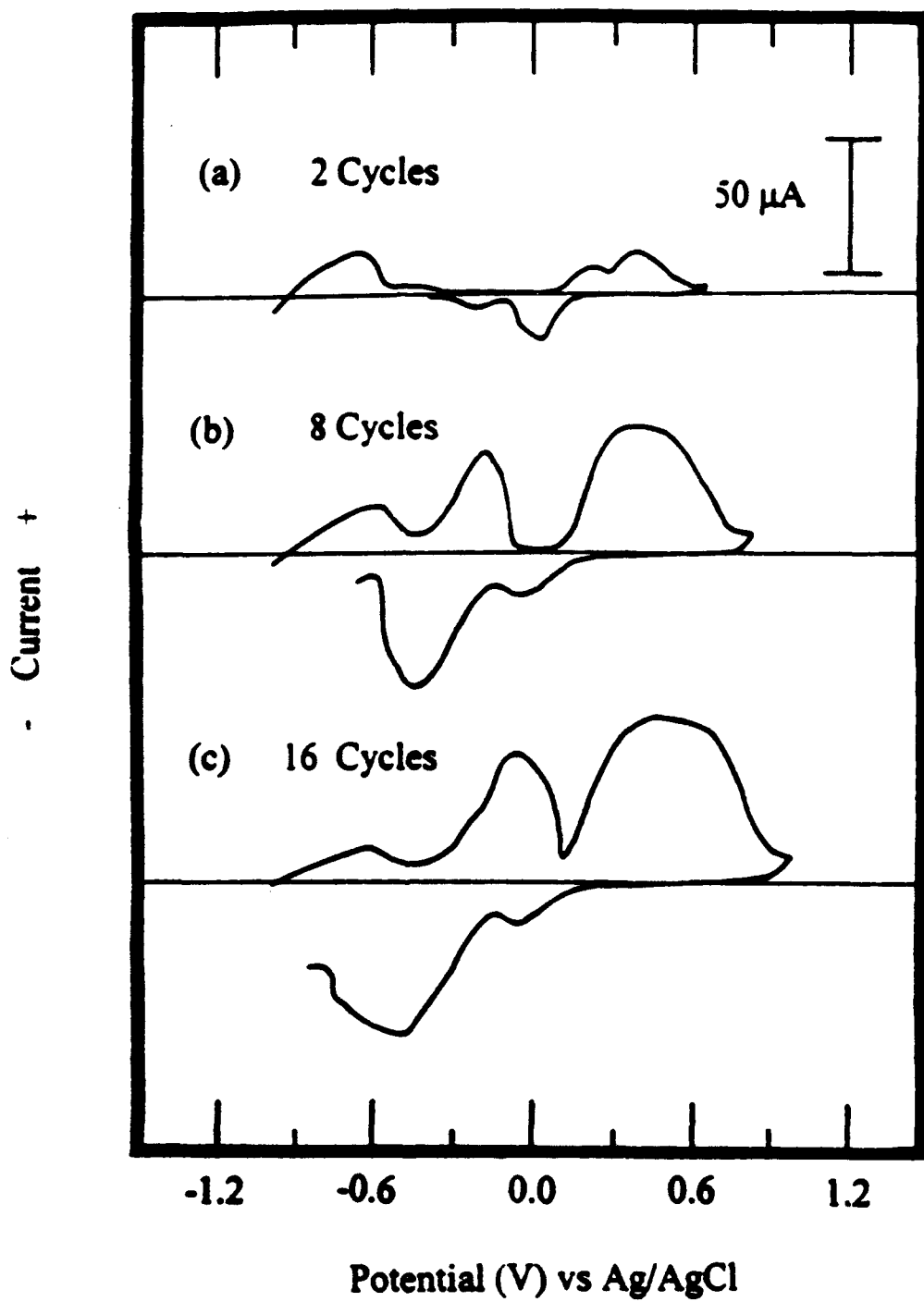


Figure 4 Choong K Rhee et. al

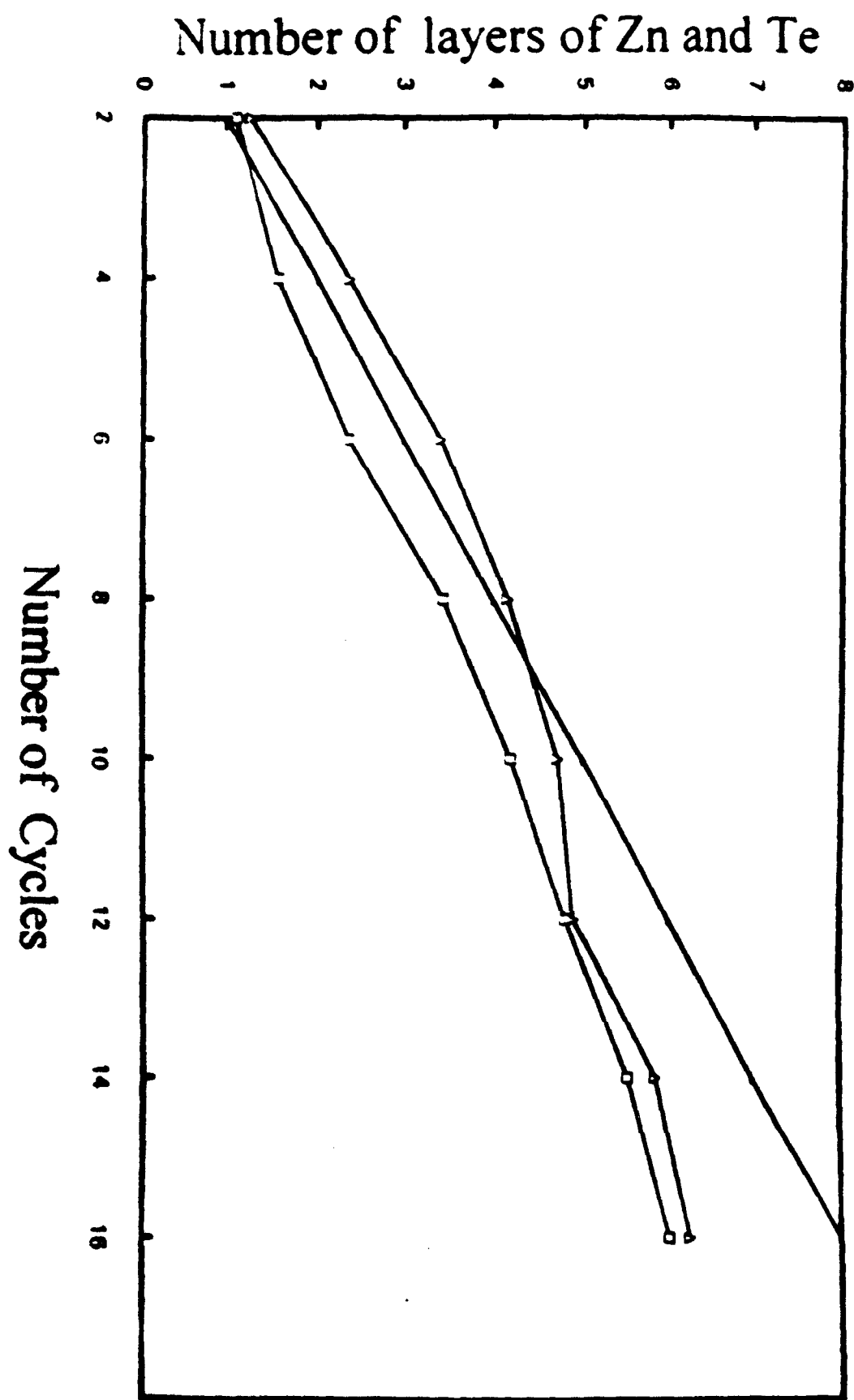


Figure 5. Choong K Rhee et. al

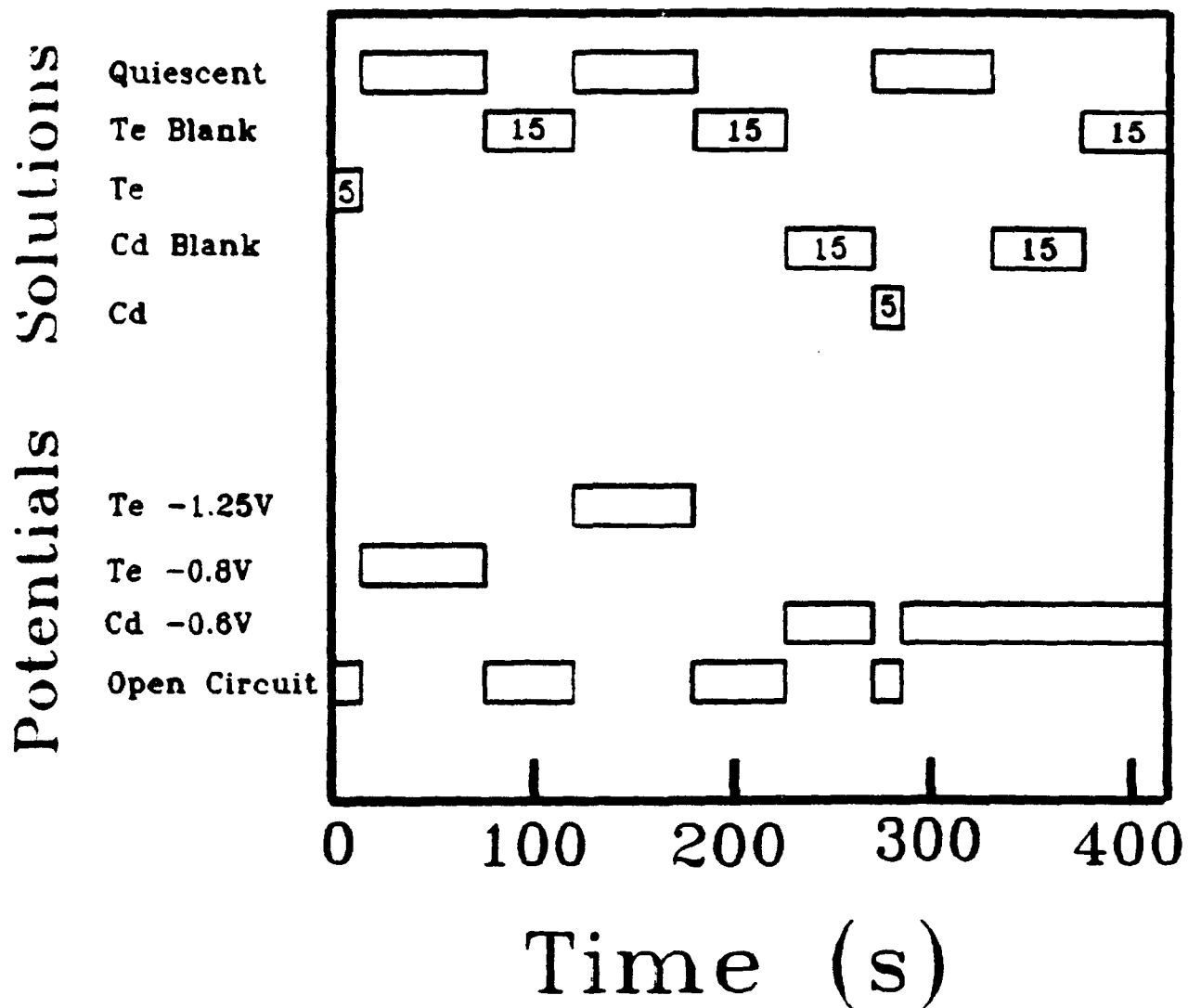


Figure 6 Choong K Rhee et. al.

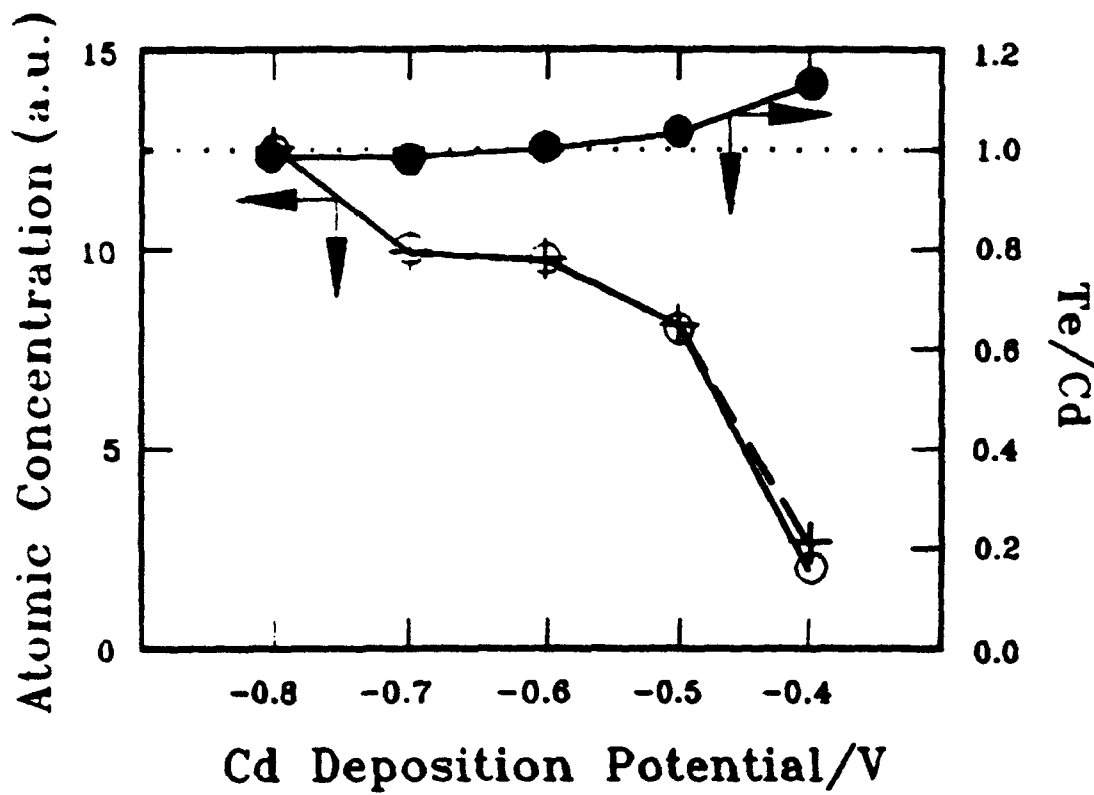


Figure 7 Choong K Rhee et al

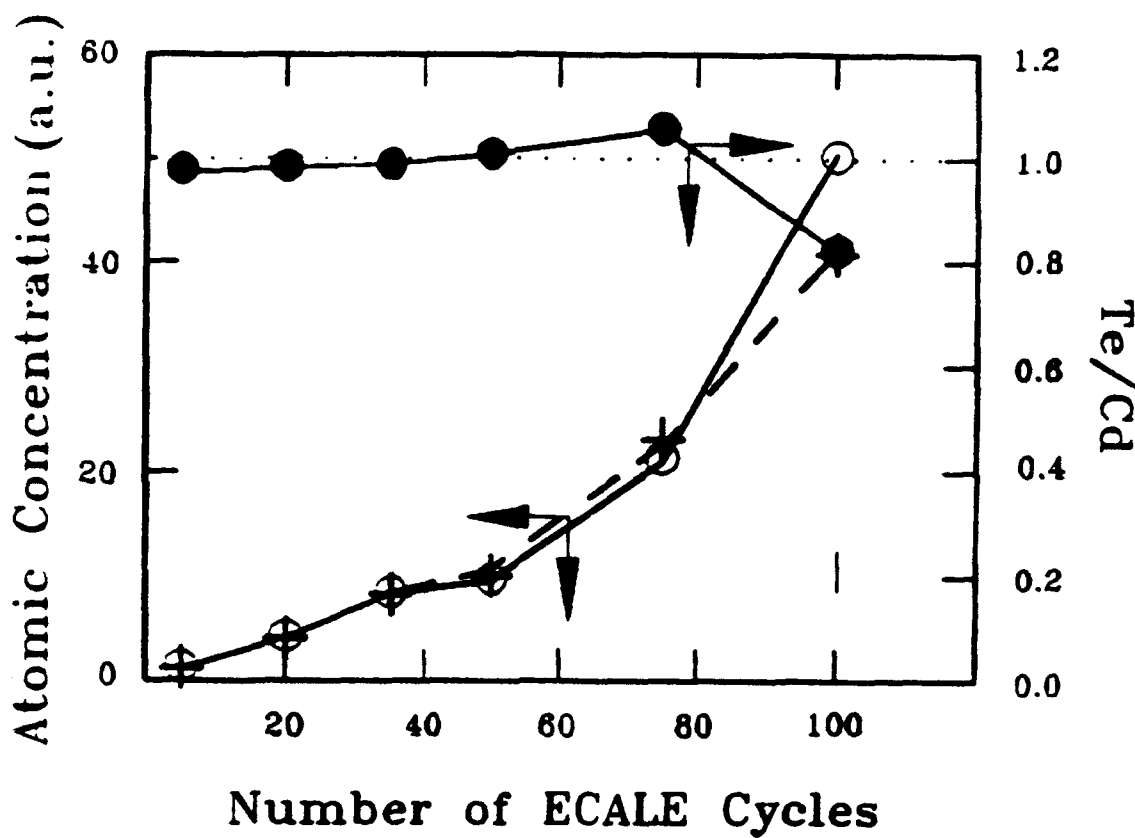


Figure 3 (a) and (b) Choong K Rhee et al



Figure 8 (c) and (d) Choong K. Rhee et al

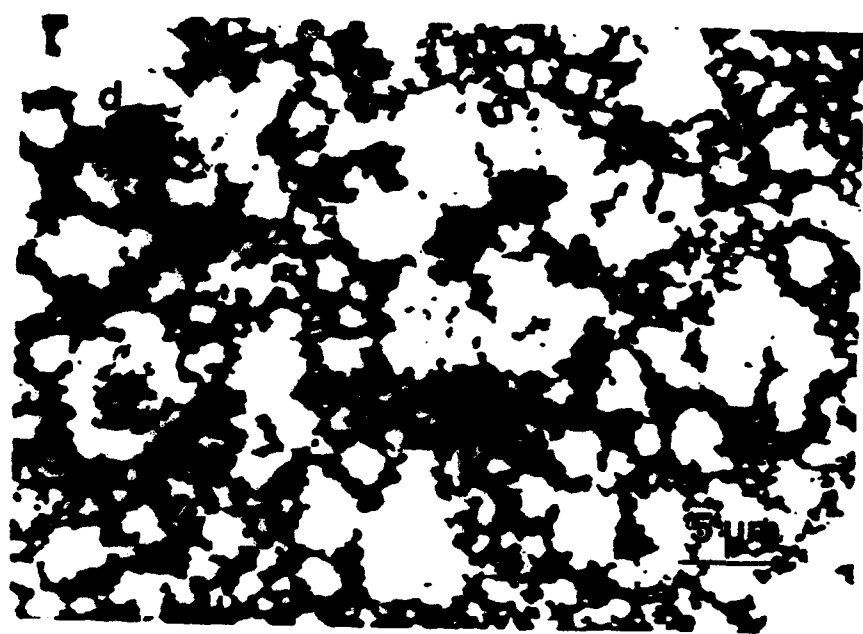


Figure 9 Choong K Rhee et al

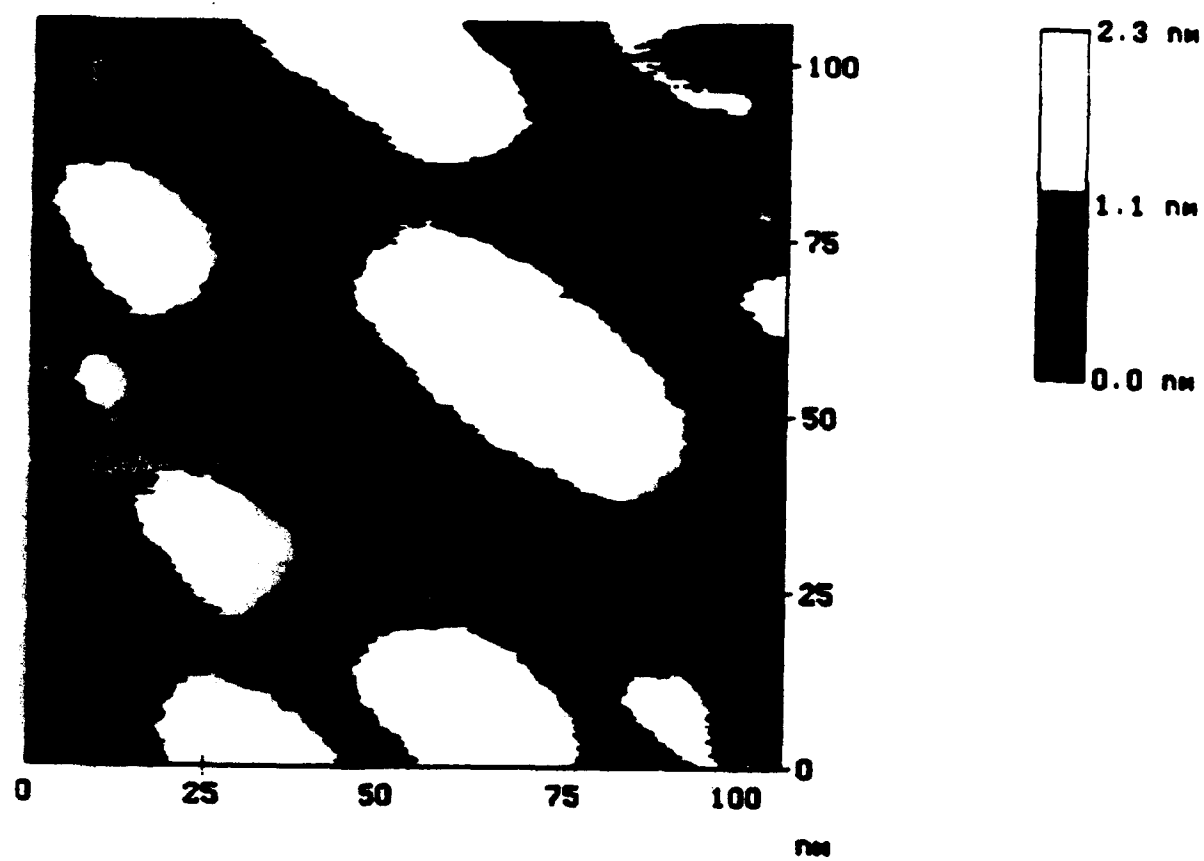


Figure 10 Choong K. Rhee et. al

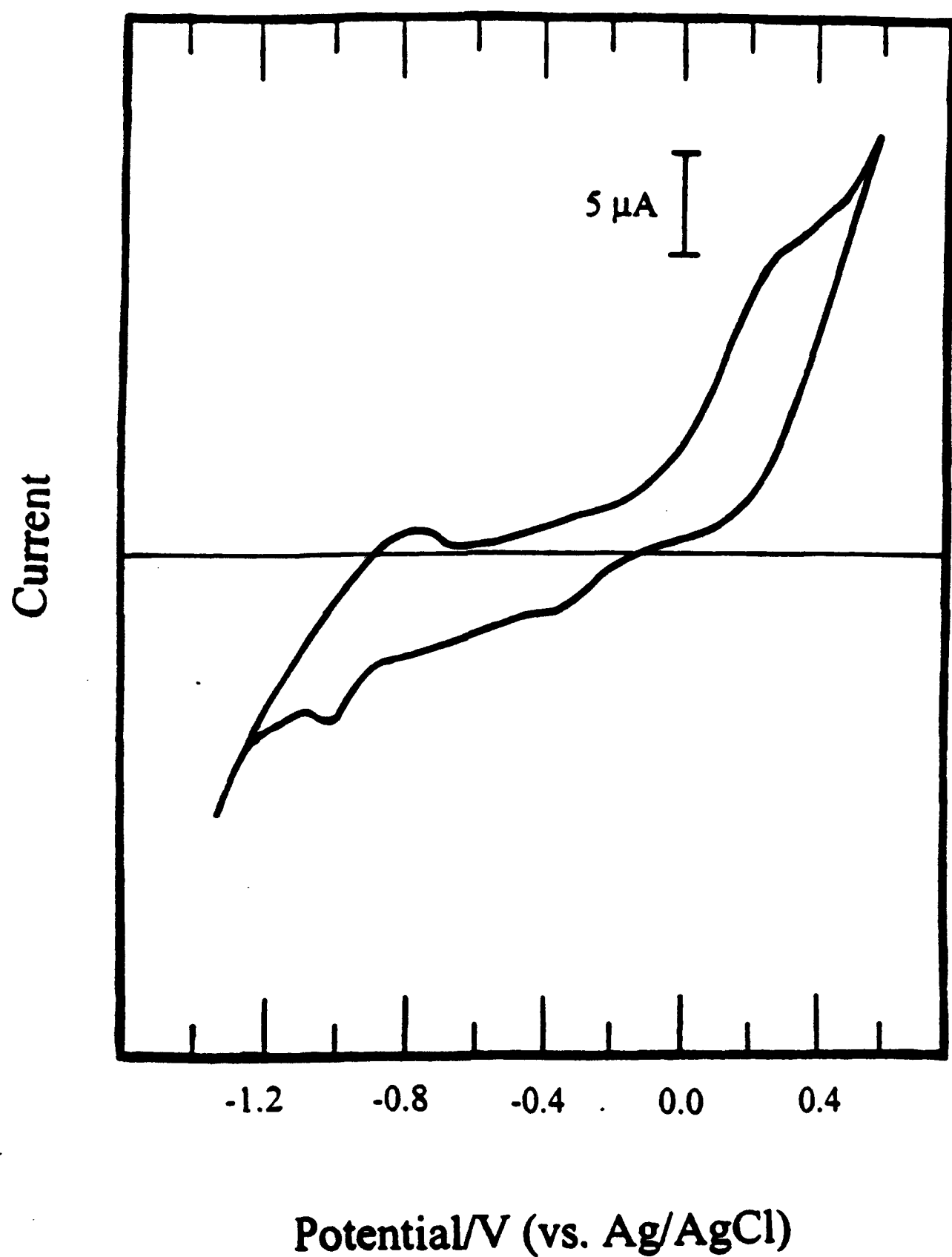


Figure 11. Choong K. Rhee et al.

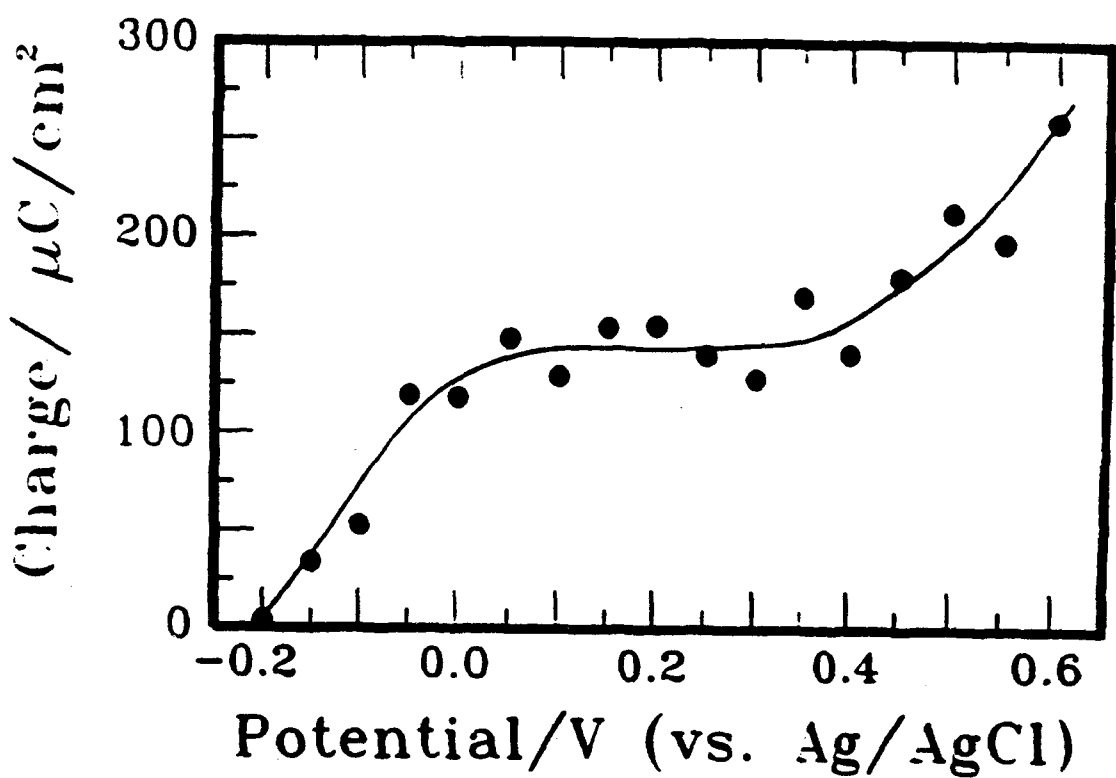


Figure 12. Choong K. Rhee et. al.

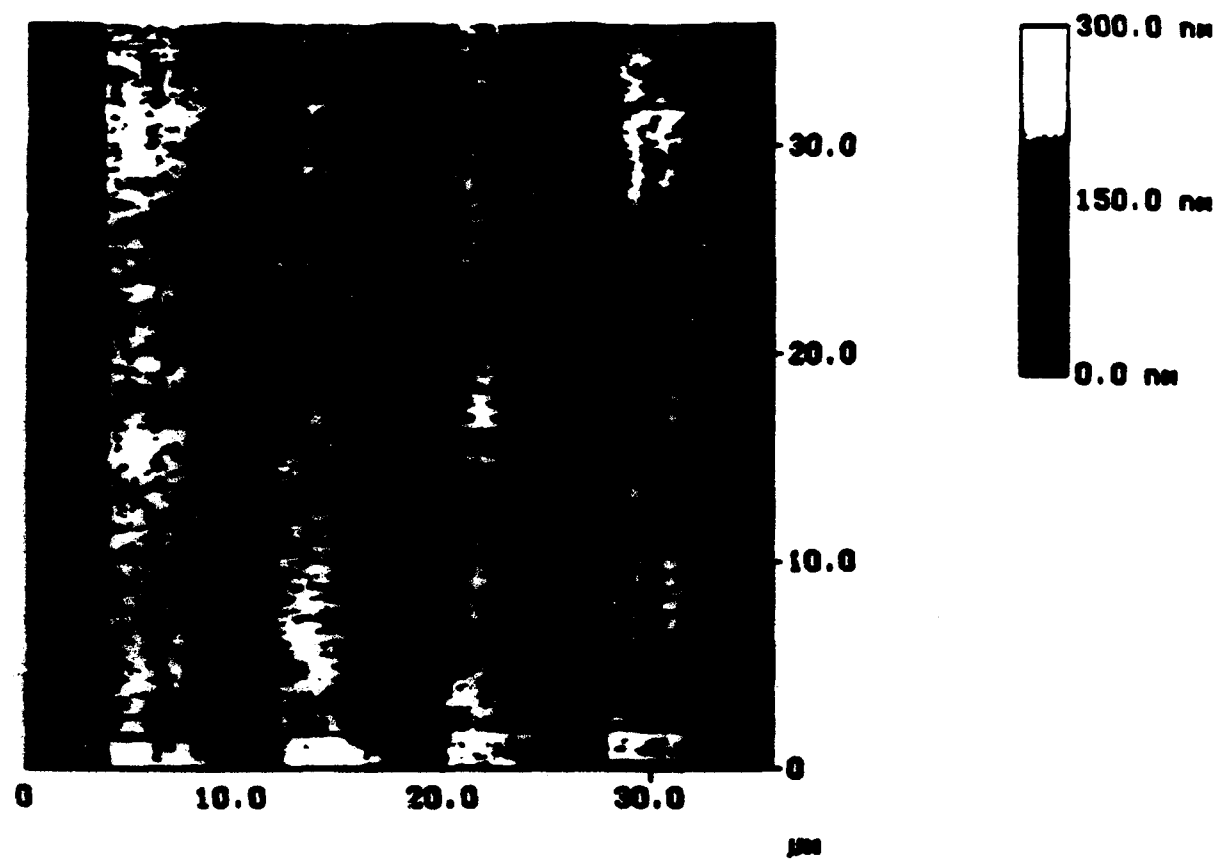


Figure 13 Choong K Rhee et al

